ACS APPLIED MATERIALS & INTERFACES

Research Article

www.acsami.org

Self-Healing Nanofiber-Reinforced Polymer Composites. 1. Tensile Testing and Recovery of Mechanical Properties

Min Wook Lee,[†] Seongpil An,[‡] Hong Seok Jo,[‡] Sam S. Yoon,*[,‡] and Alexander L. Yarin*[,†,‡]

[†]Department of Mechanical and Industrial Engineering, University of Illinois at Chicago, 842 West Taylor Street, Chicago, Illinois 60607-7022, United States

[‡]School of Mechanical Engineering, Korea University, Seoul 136-713, Republic of Korea

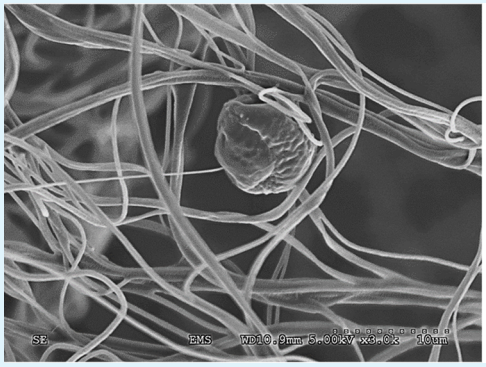

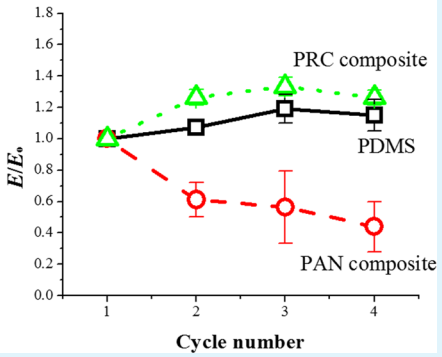

ABSTRACT: The present work aims at development of self-healing materials capable of partially restoring their mechanical properties under the conditions of prolonged periodic loading and unloading, which is characteristic, for example, of aerospace applications. Composite materials used in these and many other applications frequently reveal multiple defects stemming from their original inhomogeneity, which facilitates microcracking and delamination at ply interfaces. Self-healing nanofiber mats may effectively prevent such damage without compromising material integrity. Two types of core−shell nanofibers were simultaneously electrospun onto the same substrate in order to form a mutually entangled mat. The first type of core−shell fibers consisted of resin monomer (dimethylsiloxane) within the core and polyacrylonitrile within the shell. The second type of core−shell nanofibers consisted of cure (dimethyl−methyl hydrogen-siloxane) within the core and polyacrylonitrile within the shell. These mutually entangled nanofiber mats were used for tensile testing, and they were also encased in polydimethylsiloxane to form composites that were also subsequently subjected to tensile testing. During tensile tests, the nanofibers can be damaged in stretching up to the plastic regime of deformation. Then, the resin monomer and cure was released from the cores and the polydimethylsiloxane resin was polymerized, which might be expected to result in the self-healing properties of these materials. To reveal and evaluate the self-healing properties of the polyacrylonitrile-resin-cure nanofiber mats and their composites, the results were compared to the tensile test results of the monolithic polyacrylonitrile nanofiber mats or composites formed by encasing polyacrylonitrile nanofibers in a polydimethylsiloxane matrix. The latter do not possess self-healing properties, and indeed, do not recover their mechanical characteristics, in contrast to the polyacrylonitrile-resin-cure nanofiber mats and the composites reinforced by such mats. This is the first work, to the best of our knowledge, where self-healing nanofibers and composites based on them were developed, tested, and revealed restoration of mechanical properties (stiffness) in a 24 h rest period at room temperature.

KEYWORDS: *self-healing, core−shell nanofibers, electrospinning, composite, tensile*

1. INTRODUCTION

Self-healing is a fascinating feature exhibited by living tissues. For example, a scratch on our skin triggers the delivery of blood platelets by blood capillaries and it is soon healed. A living system detects the problem, supplies the healing agent to the damaged site, and healing occurs automatically. Self-healing in nature should happen relatively rapidly, because an open wound could result in life-threatening complications. Similar to living organisms, technically engineered materials also have a certain life expectancy; however, they do not possess any self-healing features. Therefore, time-consuming and costly inspections are frequently required to facilitate the safe operation of many engineered materials. If an undetected microcrack in an airplane body or a nuclear reactor inner-wall could be automatically repaired before it starts propagating, major disasters could be avoided. Hence, the addition of self-healing features to engineered materials and devices is an attractive subject matter for research.

Received: April 22, 2015
Accepted: August 18, 2015
Published: August 18, 2015

DOI: 10.1021/acsami.5b05998
ACS Appl. Mater. Interfaces 2015, 7, 19546−19554

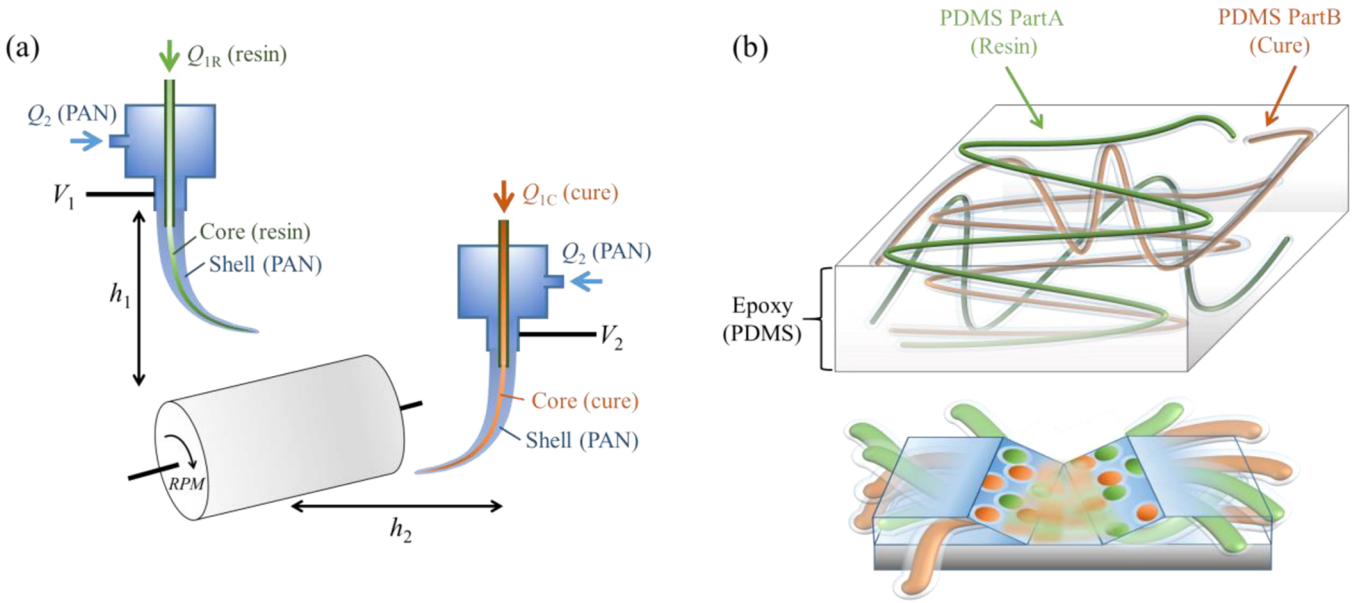

Figure 1. (a) Schematic of experimental apparatus for the simultaneous coelectrospinning of the core–shell nanofibers containing separate binary components of self-healing agent in their cores. (b) Structure of self-healing fiber-reinforced composite: core–shell nanofibers with resin monomer and cure in the core are mutually entangled and embedded in PDMS matrix; when damage occurs, resin monomer and cure are released and polymerization reaction results in PDMS-reinforced healing.

The self-healing features of engineered materials could be especially advantageous in extending the durability of their mechanical properties. Fracture is typically classified into modes I, II, and III corresponding to crack propagation under in-plane tensile stress, shear stress, and out-of-plane stress, respectively. The interfacial debonding and healing during the fracture of a composite double-cantilever beam (DCB) specimen was studied in previous research.[1−4] The DCB is one of the conventional methods of mechanical testing used in aerospace and automotive industries. The healing agent was either manually injected or embedded within the specimen for subsequent self-activation to occur. Both the crack aperture and adhesion energy required for fracture were measured in order to evaluate the effect of self-healing. A tapered double cantilever beam was also tested, and the efficiency of the self-healing properties of the sample was calculated from the changes in the critical fracture loads.[5−7] These works revealed that the employed healing methods were capable of inhibiting crack growth for mode I. The behavior of samples with self-healing features produced by vascular-like storage, which mimics the network systems of living organs was also evaluated for mode II fracture during bending.[8−12] The vascular-like storage and supply of healing agents has an advantage over the embedded capsules, however, the capillaries with sizes on the order of several millimeters are too large on a composite scale and this poses some problems. To achieve lighter composite structures, we developed ultrathin electrospun core–shell fibers containing self-healing materials within the core in previous research.[13−15] A liquid healing agent (dicyclopentadiene, DCPD) was encapsulated in the form of a core within an electrospun PAN (polyacrylonitrile) shell, producing nanofibers with a cross-sectional diameter in the order of hundreds of nanometers, while the entire thickness of the interlayer in the composite mat was estimated to be approximately 80 μm. The bending test results for these polymer matrix composites (PMCs) revealed that the strength and stiffness of the material could recover following failure. The results demonstrated that these nanofiber interlayers can be used to heal interlaminar fractures. Self-healing nanofibers were also used for anti-corrosion protection in other studies.[16,17] When an anti-corrosion coating containing such nanofibers was scratched, the two separate components of the encapsulated healing agent were supplied from the cut nanofibers and successfully healed the damaged site, thus preventing corrosion.

Composite materials used in aerospace and other applications are typically subjected to periodic loading–unloading cycles and can develop microcracking in the bulk and/or microdelamination at ply interfaces.[3,4] Even though such fatigue microcracks do not pose an immediate danger, under certain conditions they can start growing and merging, which can result ultimately in a catastrophic event. Reinforcing interfaces in composite materials by capsules with healing agents larger than 100 μm size can be ineffective, since they affect the material structure on its own (large) scale. That is the reason that electrospun nanofibers attract attention as potential reinforcing vessels of sufficiently small scale. They do not compromise material integrity and contain healing agents, which can be released in the case of microscopic cracking and/or delamination.[15] Electrospinning of monolithic nanofibers and coelectrospinning of core–shell fibers is a well-developed technique and a comprehensive exposition of the fundamental and applied aspects of this method is available in a recent monograph.[18]

In the present work, coelectrospun core–shell nanofiber mats containing two separate components of a healing agent, component A (resin, dimethylsiloxane) and component B (cure, dimethyl–methyl hydrogen-siloxane), were used to maintain the mechanical properties. The mechanical characterization of pristine, damaged, and healed composite materials was conducted by tensile testing.

2. EXPERIMENTAL SECTION

2.1. Materials. Both PAN (polyacrylonitrile, M_w = 150 kDa) and DMF (dimethylformamide, 99.8%) were purchased from Sigma-

DOI: 10.1021/acsami.5b05998
ACS Appl. Mater. Interfaces 2015, 7, 19546−19554

Table 1. Experimental Parameters

		flow rate	voltage	nozzle-to-collector distance	angular velocity of collector
core (ID: 0.61 mm/OD: 0.91 mm)	resin monomer	Q_{1R} = 0.07 mL/h	V_1 = 12−13 kV	h_1 = 10 cm	200 rpm
	cure	Q_{1C} = 0.07 mL/h	V_2 = 12−13 kV	h_2 = 10 cm	
shell (ID: 1.36 mm/OD: 1.65 mm)	PAN	Q_2 = 0.9 mL/h	as for the core	as for the core	

Aldrich. The two components of PDMS (polydimethylsiloxane, Sylgard 184), component A (resin, dimethylsiloxane) and component B (cure, dimethyl−methyl hydrogen-siloxane), were purchased from Dow Corning. Both components of the PDMS were separately supplied to the core needle of the coelectrospinning apparatus and they were embedded within the individual cores of the nanofibers, as shown in Figure 1a. The resin was diluted by *n*-hexane using a ratio of 2:1 (wt %), respectively, whereas the cure was used without further treatment. The 8 wt % PAN solution in DMF was used as the shell material. As shown in Figure 1a, for the first type of fibers, the diluted resin solution (Q_{1R}) and PAN solution (Q_2) were separately supplied as the core and shell materials, respectively. For the second type of fibers, the pure cure solution (Q_{1C}) and PAN solution (Q_2) were separately supplied as the core and shell materials. Both types of fibers were simultaneously coelectrospun on the same rotating drum, forming a mutually entangled matrix.

2.2. Coaxial Electrospinning. The core−shell nanofibers were coelectrospun from a core−shell needle following the coelectrospinning technique described in detail elsewhere.[18] Figure 1a demonstrates how the core and shell solutions were supplied to the core and shell needles with flow rates of Q_1 and Q_2, respectively. As a result, the core materials (either PDMS resin monomer, or its cure) were stored in a liquid state within the core of the core−shell fibers and each core was surrounded by the PAN shell in the separate nanofibers. As mentioned above, both types of coelectrospun nanofibers (containing either the resin monomer or cure in the core) were collected on a rotating drum collector for a period of 30 min (cf. Figure 1). The parameters for the coelectrospinning process are listed in Table 1. The illustration of the fiber-reinforced composite and the healing agent release in the damaged area are depicted in Figure 1b. It shows that the resin (green) and cure (orange) are encapsulated inside the core−shell fiber separately and the entire mutually entangled fiber mats are infiltrated with PDMS matrix. When the fibers are broken by microcracks and the encapsulated liquid agents are released, resin monomer and cure participate in polymerization reaction, which results in formation of PDMS healing links.

2.3. Fabrication of the Nanofiber-Reinforced Composite. Nanofiber mats, prepared as described above, were used to fabricate nanofiber-reinforced composites with different matrices. To prepare the composite samples for tensile testing, we cut both the nonself-healing monolithic PAN (used for comparison) and self-healing core−shell PAN-resin-cure (PRC) nanofiber mats into sections with dimensions of $l_0 \times w_0$ = 90 mm × 23 mm (cf. Figure 2a).

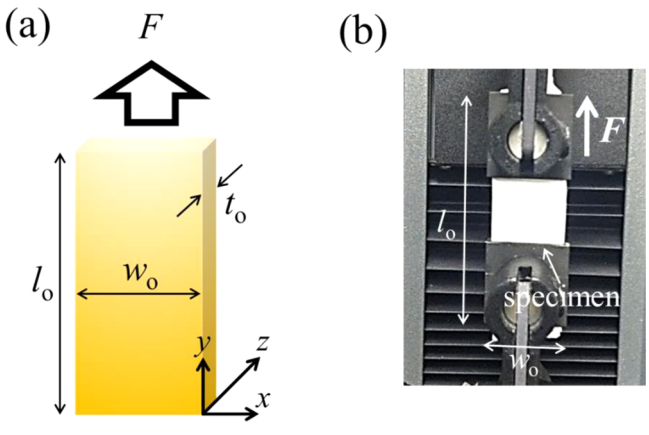

Figure 2. (a) Specimen and (b) apparatus for tensile testing.

These were sandwiched between PDMS (the premixed monomer and cure at a ratio of 10:1) as a middle layer. The PAN-to-resin volume ratio in PDMS-impregnated composites with PAN nanofibers was about 1.30% versus 1.56% in PDMS-impregnated composites with PRC nanofibers. The resulting PDMS-encased composites were cured at room temperature for 24 h. These samples were subsequently used for tensile testing (see Figure 2a). The initial thickness, t_0, of each sample was measured ten times using micrometer and the average measurement was recorded. The values of t_0 for the PAN and PRC nanofiber-reinforced composites were 0.485 and 0.425 mm, respectively. Note that such composites present significant interest as self-healing adhesive layers at the ply surfaces[19] and thus, mechanical testing of thin samples should be attempted.

It should be emphasized that PDMS matrices of the prepared composites can be damaged (develop multiple microcracks) during stretching of samples made of them, as it happens with matrices of many other composites used in the aerospace and other industries. However, in the present case, the PDMS matrices embed mutually entangled core−shell nanofibers containing resin monomer and cure in their cores. These nanofibers are also expected to be damaged during stretching. They will then release resin monomer and cure into the surrounding microcracks of the PDMS matrix. As a result, polymerization of the released resin in the presence of cure will happen and PDMS links spanning banks of microcracks in the PDMS matrix will be formed. This is the self-healing mechanism that will be explored in the following sections.

2.4. Tensile Testing. The standard in tensile testing of nanofiber mats was established in the previous works of the present group[18,20−23] and followed here. The PDMS-encased composite samples, prepared as described in section 2.3, were employed during tensile testing, using an Instron 5942. The initial sample length between the upper and lower grips was set to 20 mm (cf. Figure 2b). During the experiments, the stretching rate was set as 1 mm/min. It should be emphasized that such low stretching rates are characteristic of many industrial applications where the accumulation of the mechanically generated microcracks happens relatively slowly before it suddenly results in a catastrophic event. The acquired data were presented in the form of stress−strain curves.

The procedure described below was used to evaluate the self-healing features of the PDMS-encased samples containing the self-healing core−shell PAN-resin-cure (PRC) nanofibers. The samples were stretched to a strain of 15−18%, which resulted in internal damage. The accumulated damage at such strains was revealed during the experiments on the PDMS-encased samples containing non-self-healing PAN nanofibers; these samples did not recover the original stress−strain curve, as discussed below in section 3.2. The PDMS-encased samples with self-healing core−shell PRC nanofibers were left for 24 h to ensure that polymerization of the released resin monomer occurred when it came in contact with cure that was released from the damaged nanofibers. Subsequently, the samples were used for further tensile testing to evaluate whether the previous stress−strain curve would recover (which implies full self-healing) or not. The results are discussed in section 3.2.

2.5. Optical Characterization. The morphology of the core−shell fibers and elemental analysis of the encapsulated healing agents were studied using SEM/EDX (Hitachi S-3000N) at 5 kV. The fiber diameter was found using at least 100 measurements for a proper statistics. To reveal the core−shell structure of the fibers and resin and cure encapsulation in the PAN shell, we employed TEM (transmission electron microscopy using JEM 2100F, JEOL Inc.) under 200 kV operating condition.

DOI: 10.1021/acsami.5b05998
ACS Appl. Mater. Interfaces 2015, 7, 19546−19554

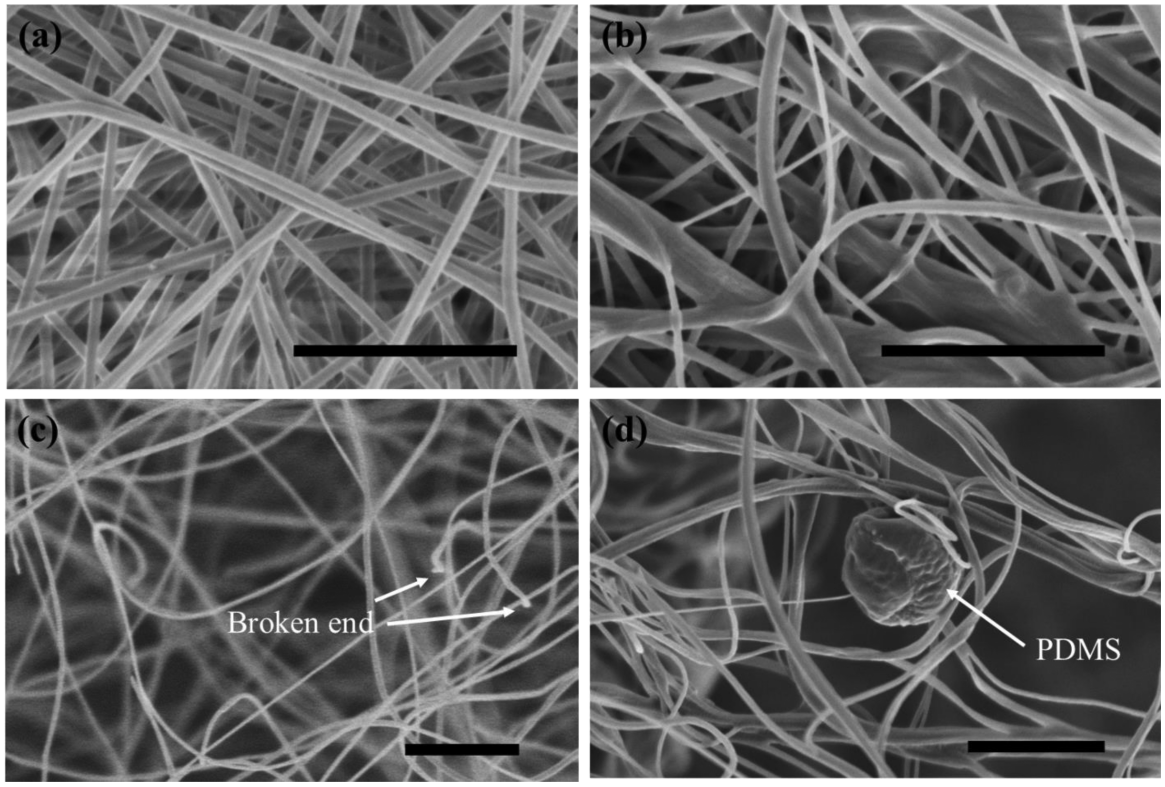

Figure 3. SEM image of pristine fiber mats: (a) PAN nanofiber mat, (b) self-healing PRC. The same mats following the repeated (third) tensile test under regime II (discussed below): (c) PAN mat with a fiber diameter of approximately 544 ± 180 nm, (d) PAN-resin-cure (PRC) nanofiber mat, with an average fiber diameter of 578 ± 138 nm. The scale bars are 10 μm.

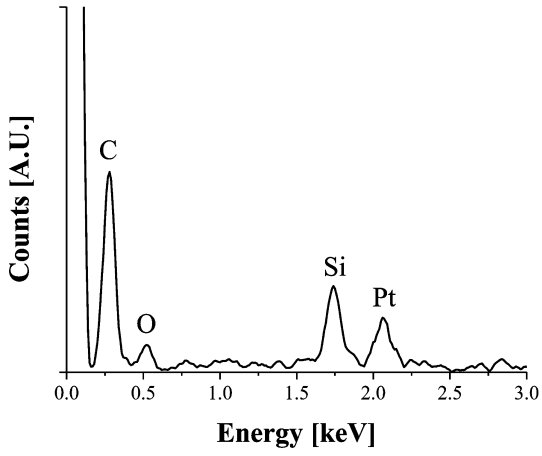

Element	Weight %	Atomic %
C K	52.81	81.54
O K	7.94	9.20
Si K	9.78	6.46
Pt M	29.47	2.80
Total	100.00	100.00

Figure 4. EDX analysis of the spherical mass observed in Figure 3d.

3. RESULTS AND DISCUSSION

3.1. Morphology and Elemental Analysis of the Released Material. The scanning electron microscopy (SEM) images of the pristine nanofiber mats are shown in Figures 3a (the PAN mat) and 3b (the self-healing PRC mat). The corresponding SEM images of the mats following tensile testing are exhibited in Figure 3c, d, respectively. The PAN nanofibers in Figure 3a are uniform with a fiber cross-sectional diameter of 588 ± 135 nm. Furthermore, in the pristine self-healing PRC mat, fibers with two different diameters can be distinguished, namely, 1.32 ± 0.50 μm and 373 ± 105 nm; these are the fibers with the resin monomer and cure within the core, respectively, as demonstrated in Figure 3b. Following the repeated (third) tensile test (discussed in detail in relation to Figure 6 below), it can be observed that some of the originally straight PAN nanofibers were broken and the suspended edges of these broken fibers exhibited a curled appearance (cf. Figure 3c). Moreover, the fiber diameter decreased from 588 ± 135 nm to 544 ± 180 nm. As shown in Figure 3d, the self-healing PRC fibers also became tortuous, and spherical masses of released and polymerized PDMS emerged from the fibers. The average diameter of the fibers was 578 ± 138 nm.

It should be emphasized that it was shown before that the fiber mat thicknesses do not reveal any definite dependence on the fiber deposition time.[24] In particular, it was shown that as the fiber mat thickness may stay constant or even diminish, the

DOI: 10.1021/acsami.5b05998
ACS Appl. Mater. Interfaces 2015, 7, 19546−19554

pore size diminishes at longer deposition times, which corresponds to a denser packing of nanofibers.

The elemental composition of the released spherical mass (that can be observed in Figure 3d) was analyzed using energy-dispersive X-ray spectroscopy (EDX). As exhibited in Figure 4, the EDX analysis results revealed a clearly recognizable silicon (Si) peak at an energy of approximately 1.8 keV, which indicates that the released material consists of PDMS.

The presence of the solid mass illustrates the fact that the PDMS-resin monomer was released from a broken fiber. This PDMS-resin monomer came into contact with the cure released from another broken fiber, and polymerization occurred at the site of the broken fiber. As expected, such PDMS masses function as a glue, adhering the broken fibers to the entire fiber mat. It should be emphasized that a peak corresponding to platinum (Pt) was detected by the EDX analysis because the sample had been sputtered with platinum for improved SEM imaging.

In addition, transmission electron microscopy was employed to directly observe the core inside the core–shell nanofibers. The results shown in Figure 5 reveal the core–shell structure and collaborate the findings of the EDX analysis.

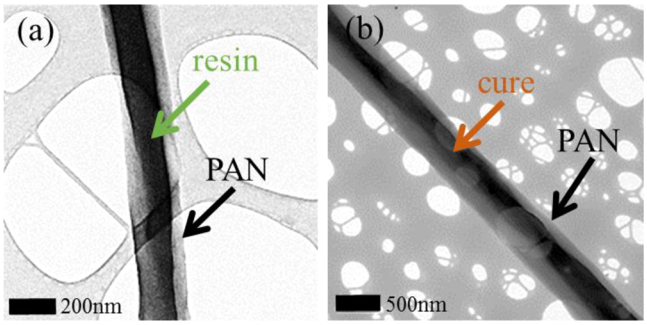

Figure 5. TEM images of core–shell nanofibers: (a) resin-PAN fiber, and (b) cure-PAN fiber.

3.2. Self-Healing Phenomena during Tensile Testing.

Figure 6 shows the tensile test results for both the PAN mat and the self-healing PRC fiber mat. The thicknesses of the PAN and PAN-resin-cure fiber mats were 0.089 mm and 0.191 mm, respectively, which indicates that the PAN-resin-cure sample is 2.15 times thicker than the PAN sample. This is because the two additional components (PDMS resin monomer and cure) were simultaneously supplied with the PAN solution during the coelectrospinning process. The Young's moduli, E, of the PAN mat and the self-healing PRC fiber mat samples were 46.45 and 18.05 MPa, respectively. This indicates that the PAN nanofiber mat, which is fully solidified, is stiffer than the self-healing PRC fiber mat containing the liquid resin monomer or cure within the fiber cores. The ultimate tensile strength of the PAN nanofiber mat is also twice that of the self-healing PRC fiber mat.

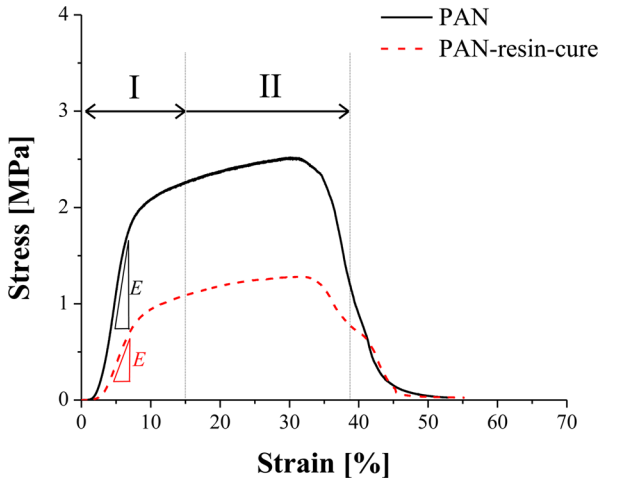

Figure 6. Stress–strain curves measured during tensile testing of the PAN and PAN-resin-cure fiber mats.

The results revealed the following recognizable well-defined regimes of deformation within the stress–strain curves. Namely, elastic regime, where the stress–strain dependences are linear; intermediate plastic regime, where the dependences are nonlinear; and the ultimate catastrophic failure. These regimes are typical for the different nanofiber mats.[20−23]

Figure 7 shows the results of repeated tensile tests that encompass a strain range up to 15% (elastic regime and the initial part of plastic regime) for both the PAN and PAN-resin-cure (PRC) fiber mats. Stretching up to 15% (deep into the irreversible plastic regime) results in moderately damaged mats. Each mat was initially stretched and allowed to rest for 24 h prior to tensile testing. Each mat was subjected to four sequential tensile tests. Figure 7a reveals that the PAN nanofiber mat exhibited deterioration in the mechanical properties immediately after the first tensile test. Indeed, during the second tensile test, the stress–strain curve even revealed catastrophic failure at a strain of 7.5%. During the sequential tensile tests, the PAN sample exhibits only a slight resistance to stretching and the stiffness and the ultimate strength significantly decline during the repeated tests. Conversely, during the four sequential tensile tests, the self-healing PRC sample reveals stress–strain curves which are pretty similar to each other (cf. Figure 7b). In Figure 7c, the Young's moduli measured during the sequential tests are normalized by the result obtained during the first test. The dependences for the PAN mat (black open squares) and the self-healing PRC (red open circles) are drastically different. During the fourth sequential tensile test, the Young's modulus decreased (relative to its original value) by 90% for the PAN mat, but just by 30% for the self-healing PRC sample. Specifically, the sample was healed by the release of the resin monomer and cure that were stored separately within the nanofiber cores. It should be emphasized that the PAN nanofiber mat was significantly weakened during the sequential testing and completely failed during the fourth tensile test, in contrast to the self-healing PRC sample, as shown in Figure 7d.

In addition to the sequential tensile testing up to a strain of 15%, as illustrated in Figure 7, similar tests were conducted by stretching the samples to the level related to catastrophic failure (up to 30% strain). The corresponding results are presented in Figure 8. As Figure 8d illustrates,during these tests the stretched fiber mats significantly shrunk in the middle, which is contrasted by comparison with the sample shown in Figure 7d. It should be emphasized that the samples shown in Figures 7d and 8d underwent different strain regimes. The sample shown in Figure 7d underwent repeated stretching in moderate strain range (regime I, strains up to $\varepsilon \approx 15\%$), whereas the sample shown in Figure 8d was stretched beyond failure (regime II, strains up to $\varepsilon \approx 30\%$). The plastic deformation during the tensile test in regime II results in the dog-bone shape

DOI: 10.1021/acsami.5b05998
ACS Appl. Mater. Interfaces 2015, 7, 19546−19554

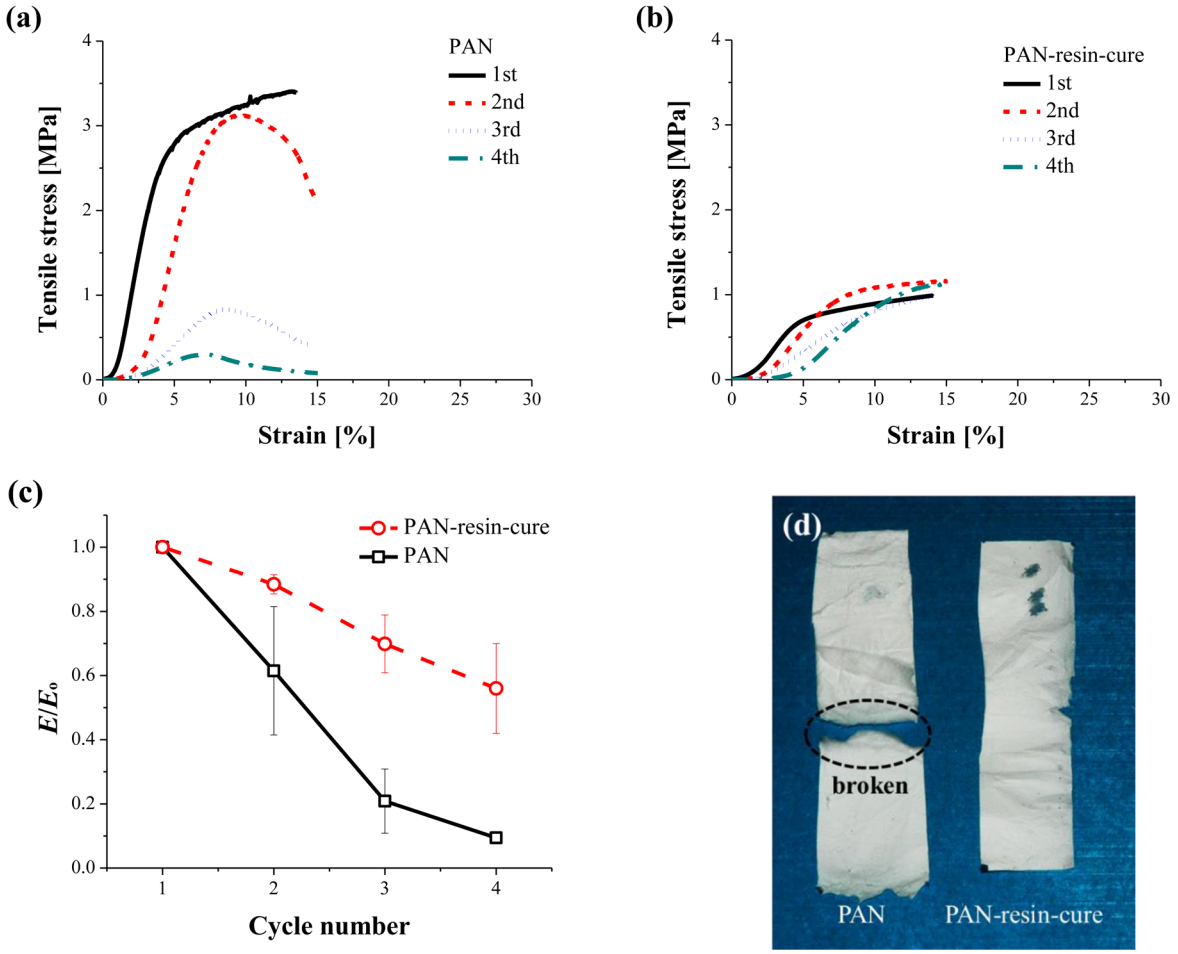

Figure 7. Stress−strain curves measured during tensile testing with a strain range of 15% (elastic regime I and the initial part of plastic regime II). (a) PAN nanofiber mat, (b) PAN-resin-cure fiber mat. (c) Relative variation in the Young's modulus during the repeated tests. (d) Images of the samples following the repeated tensile testing.

in the middle of the strip characteristic of many materials in such situations.

Notably, the self-healing PRC sample revealed similar behavior to that of the PAN sample (observed by comparing Figure 8a, b). The self-healing sample only slightly outperforms the pure PAN sample, as shown in Figure 8c. Indeed, the normalized values of the Young's modulus for the self-healing PRC material are only 11 and 15% greater than that of the pure PAN sample during the second and third tensile tests, respectively. The results for the experiments with the extensive sequential stretching imply that the broken sections of the nanofibers are separated to such an extent during these experiments, that self-healing becomes practically impossible, even though the PDMS resin monomer and cure are released from the cores of the broken fibers.

3.3. Tensile Testing of the PDMS Composites with PAN and Self-Healing PRC Nanofibers. The PDMS-impregnated composite with PRC (self-healing) nanofibers was subjected to tensile testing. The composite samples were subjected to tensile tests every 24 h, up to a strain of 15−18%. The Young's modulus measured during the first stretching is denoted as E_0, whereas those measured during the sequential stretching tests of the same sample are denoted as E. Figure 9 shows that the relative values of E/E_0 for the PRC (self-healing) composite samples contrast with those of both the pure PDMS samples and the PAN-nanofiber-based composite samples. The pure PDMS samples were used as a reference case, and their Young's modulus values were relatively unchanged during the four sequential tensile tests. This correlates with the results of previous research,[25] where the stress−strain curve of a PDMS sample (up to 50% strain) was almost the same as the initial curve following ten tensile tests. In general, PDMS is regarded as a good elastomer.

Figure 8c shows that stiffness of the PDMS composite with self-healing PRC fibers is not only sustained but is even increased following the repeated tensile tests. Indeed, following the fourth test, the Young's modulus of such composites increased by a factor of 1.4 compared to the initial result. This implies that both the resin monomer and cure were released from the damaged fiber cores and they not only healed the composite but even strengthened it. The healing PDMS resin is identical to that of the matrix, which facilitates their compatibility. Furthermore, the composite containing PAN nanofibers reveals a significant deterioration of its stiffness during the repeated tensile tests.

It should be emphasized that the comparison between monolithic PAN and PRC core−shell fiber mats and the composites that embed them is based not on their respective stiffness but on the respective ability to restore the original stiffness after repeated moderate stretching or a single stretching up to a catastrophic plastic deformation. Therefore, the differences observed between monolithic PAN nanofiber

DOI: 10.1021/acsami.5b05998
ACS Appl. Mater. Interfaces 2015, 7, 19546−19554

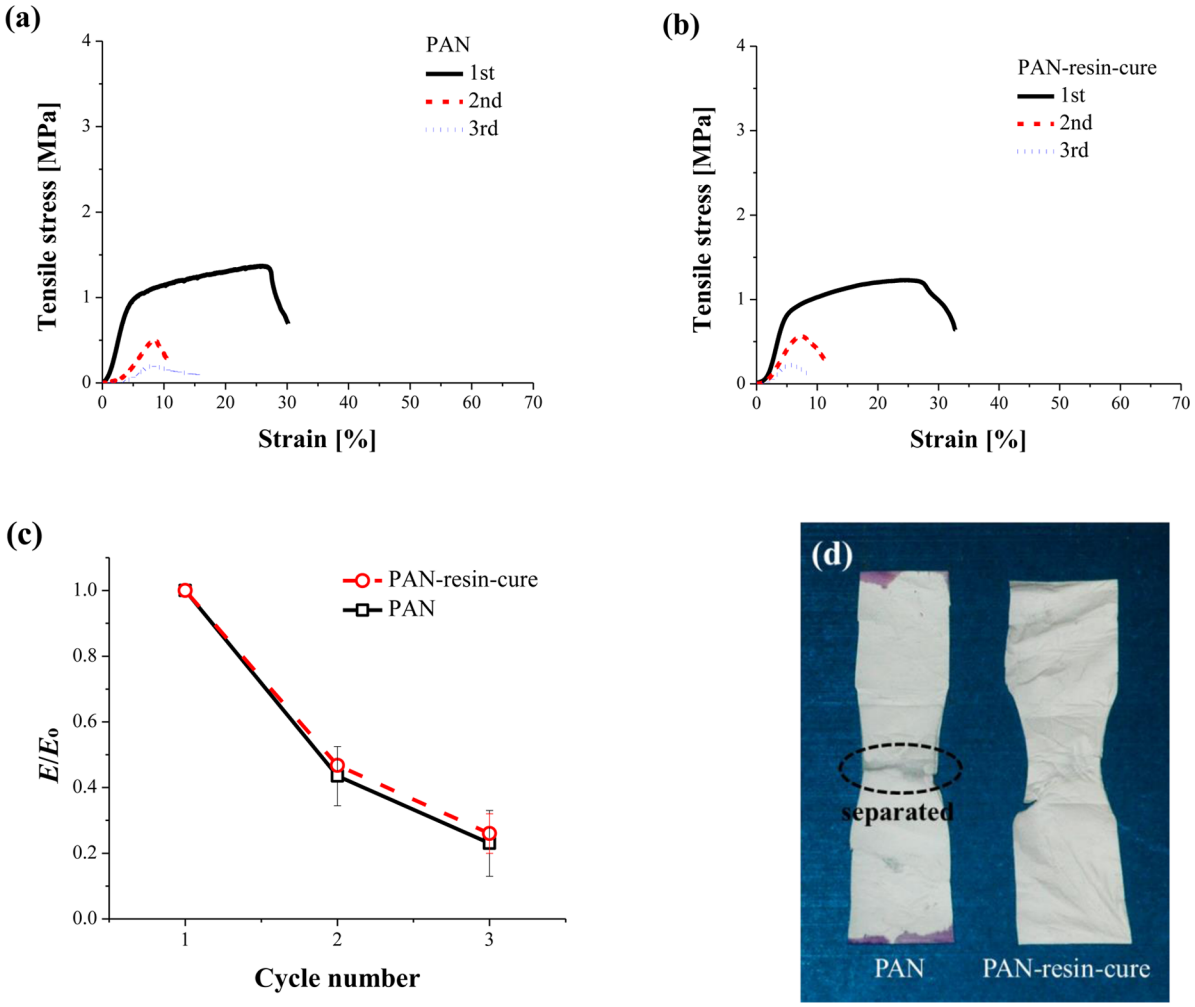

Figure 8. Stress–strain curves measured during tensile testing in the strain range of 30% (catastrophic failure, regime III). (a) PAN nanofiber mat, (b) PAN-resin-cure fiber mat. (c) Relative variation of the Young's modulus during the repeated tests. (d) Images of the samples following repeated tensile testing.

mats and PRC fiber mats (as well as their respective composites) can be safely attributed only to the effect of the healing agents released from the damaged cores of self-healing PRC fibers.

Note also that restoration of mechanical properties in a 24 h rest period at room temperature demonstrated in the present work is an attractive result that fully corresponds to the practical requirements. Indeed, in airplanes fatigue microcracks accumulate for years, and their partial every-day healing could probably prevent such catastrophic events as opening a "football-sized" hole in the fuselage, as it happened in 2009 and 2011 on commercial flights.[26] Some other published results reveal self-healing caused by different agents encased in capsules after the rest periods of 24–48 h at elevated temperatures.[3,4]

4. CONCLUSIONS

Resin monomer and cure were released from the cores of PAN-resin-cure (PRC) nanofiber mats that were damaged by tensile tests. In addition, SEM images and EDX analysis revealed that polymerized PDMS masses formed in these materials function as a glue, adhering the broken fibers to the entire nanofiber mat and the surrounding PDMS matrix. The self-healing properties of the PRC nanofiber mats and PDMS-based composites reinforced by such mats facilitated the restoration of the mechanical properties, as demonstrated by the results of sequential tensile tests with up to 15% strain accompanied by irreversible plastic deformation. Beyond this strain, the plastic deformations become so large that the broken sections of the nanofibers are separated to the distances at which self-healing becomes practically impossible, regardless of the fact that the PDMS resin monomer and cure are still released from the cores of the broken fibers.

The strength of PRC nanofiber mats and their composites is not immediately restored, as a 24 h rest period is required for the completion of the polymerization reaction. The restoration of the original mechanical properties (Young's modulus) was revealed during experiments on nanofiber mats that were subjected to four sequential tensile tests. Moreover, the self-healing PRC samples revealed relatively identical stress–strain curves as demonstrated in all four sequential tensile tests. Nanofiber mats of monolithic PAN nanofibers and their composites were used for comparison as an example of nonself-healing materials; these samples deteriorated after the first tensile test. Conversely, the PDMS-impregnated composites with PRC revealed self-healing properties during tensile testing.

DOI: 10.1021/acsami.5b05998
ACS Appl. Mater. Interfaces 2015, 7, 19546–19554

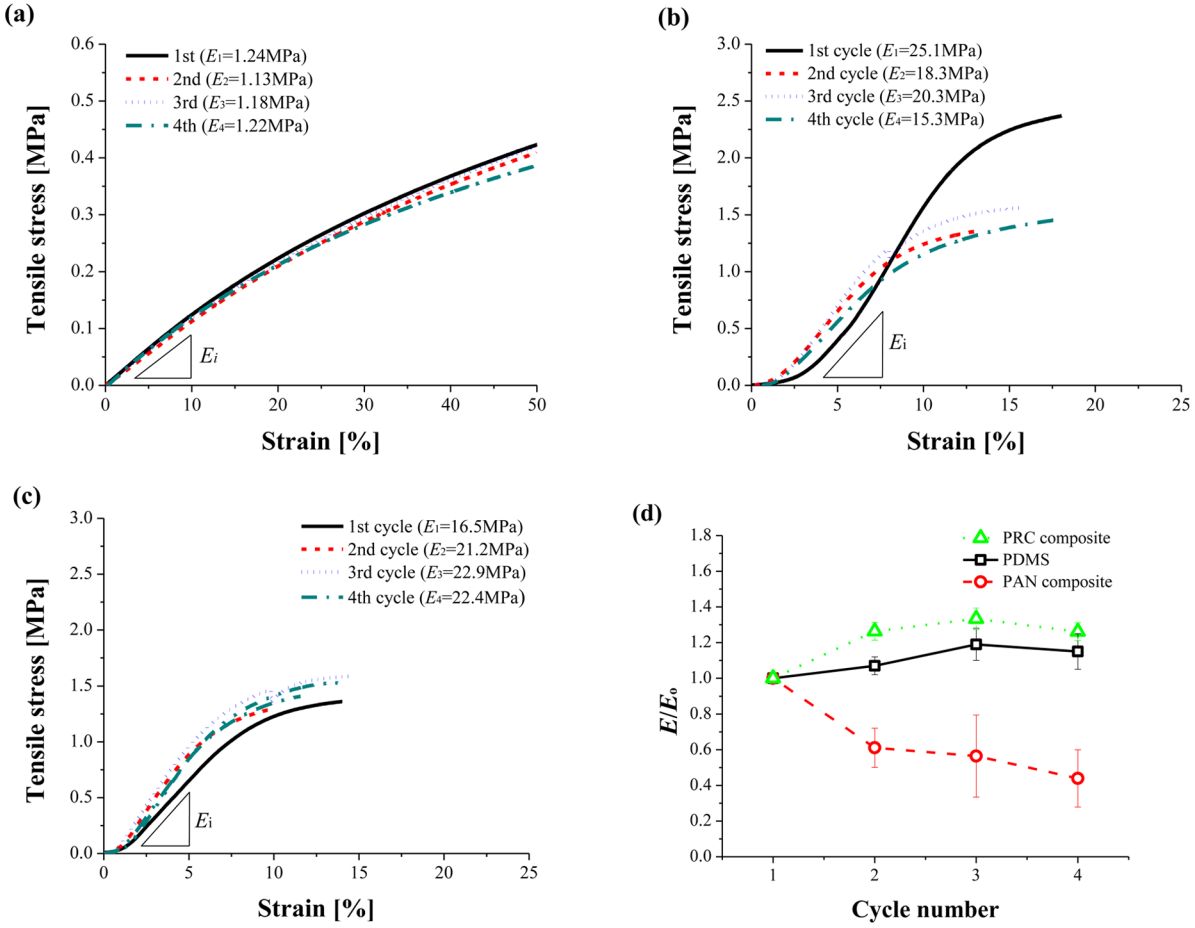

Figure 9. Stress–strain curves of (a) pure PDMS, (b) PAN-based composites, and (c) PCR (PAN-resin-cure) self-healing composites; (d) relative Young's moduli.

AUTHOR INFORMATION

Corresponding Authors

*E-mail: ayarin@uic.edu. Phone: (312) 996-3472. Fax: (312) 413-0447.

*E-mail: skyoon@korea.ac.kr. Phone: +82-2-3290-3376. Fax: +82-2-926-9290.

Notes

The authors declare no competing financial interest.

ACKNOWLEDGMENTS

This work was primarily supported by the International Collaboration Program funded by the Agency for Defense Development. This work was partially supported by ISTDP (10045221), GFHIM (NRF-2013M3A6B1078879), and NRF-2013R1A2A2A05005589.

REFERENCES

(1) Kessler, M. R.; White, S. R. Self-Activated Healing of Delamination Damage in Woven Composites. *Composites, Part A* **2001**, *32*, 683–699.

(2) Kessler, M. R.; Sottos, N. R.; White, S. R. Self-Healing Structural Composite Materials. *Composites, Part A* **2003**, *34*, 743–753.

(3) Coope, T. S.; Mayer, U. F. J.; Wass, D. F.; Trask, R. S.; Bond, I. P. Self-Healing of an Epoxy Resin Using Scandium(III) Triflate as a Catalytic Curing Agent. *Adv. Funct. Mater.* **2011**, *21*, 4624–4631.

(4) Coope, T. S.; Wass, D. F.; Trask, R. S.; Bond, I. P. Metal Triflates as Catalytic Curing Agents in Self-Healing Fibre Reinforced Polymer Composite Materials. *Macromol. Mater. Eng.* **2014**, *299*, 208–218.

(5) Brown, E. N.; White, S. R.; Sottos, N. R. Microcapsule Induced Toughening in a Self-Healing Polymer Composite. *J. Mater. Sci.* **2004**, *39*, 1703–1710.

(6) Brown, E. N.; Sottos, N. R.; White, S. R. Fracture Testing of a Self-Healing Polymer Composite. *Exp. Mech.* **2002**, *42* (4), 372–379.

(7) White, S. R.; Sottos, N. R.; Geubelle, P. H.; Moore, J. S.; Kessler, M. R.; Sriram, S. R.; Brown, E. N.; Viswanathan, S. Autonomic Healing of Polymer Composites. *Nature* **2001**, *409*, 794–797.

(8) Williams, H. R.; Trask, R. S.; Bond, I. P. Self-Healing Composite Sandwich Structures. *Smart Mater. Struct.* **2007**, *16*, 1198–1207.

(9) Toohey, K. S.; Sottos, N. R.; Lewis, J. A.; Moore, J. S.; White, S. R. Self-Healing Materials with Microvascular Networks. *Nat. Mater.* **2007**, *6*, 581–585.

(10) Pang, J. W. C.; Bond, I. P. A Hollow Fibre Reinforced Polymer Composite Encompassing Self-Healing and Enhanced Damage Visibility. *Compos. Sci. Technol.* **2005**, *65*, 1791–1799.

(11) Trask, R. S.; Bond, I. P. Biomimetic Self-Healing of Advanced Composite Structures Using Hollow Glass Fibres. *Smart Mater. Struct.* **2006**, *15*, 704–710.

(12) Williams, G.; Trask, R.; Bond, I. A Self-Healing Carbon Fibre Reinforced Polymer for Aerospace Applications. *Composites, Part A* **2007**, *38*, 1525–1532.

(13) Wu, X.-F.; Rahman, A.; Zhou, Z.; Pelot, D. D.; Sinha-Ray, S.; Chen, B.; Payne, S.; Yarin, A. L. Electrospinning Core-Shell Nanofibers for Interfacial Toughening and Self-Healing of Carbon-Fiber/Epoxy Composites. *J. Appl. Polym. Sci.* **2013**, *129*, 1383–1393.

(14) Sinha-Ray, S.; Pelot, D. D.; Zhou, Z. P.; Rahman, A.; Wu, X.-F.; Yarin, A. L. Encapsulation of Self-Healing Materials by Coelectrospinning, Emulsion Electrospinning, Solution Blowing and Intercalation. *J. Mater. Chem.* **2012**, *22*, 9138–9146.

DOI: 10.1021/acsami.5b05998
ACS Appl. Mater. Interfaces 2015, 7, 19546–19554

(15) Wu, X.-F.; Yarin, A. L. Recent Progress in Interfacial Toughening and Damage Self-Healing of Polymer Composites Based on Electrospun and Solution-Blown Nanofibers: An Overview. *J. Appl. Polym. Sci.* **2013**, *130*, 2225−2237.
(16) Lee, M. W.; An, S.; Lee, C.; Liou, M.; Yarin, A. L.; Yoon, S. S. Self-Healing Transparent Core-Shell Nanofiber Coatings for Anti-Corrosive Protection. *J. Mater. Chem. A* **2014**, *2*, 7045−7053.
(17) Lee, M. W.; An, S.; Lee, C.; Liou, M.; Yarin, A. L.; Yoon, S. S. Hybrid Self-Healing Matrix Using Core−Shell Nanofibers and Capsuleless Microdroplets. *ACS Appl. Mater. Interfaces* **2014**, *6*, 10461−10468.
(18) Yarin, A. L.; Pourdeyhimi, B.; Ramakrishna, S. *Fundamentals and Applications of Micro- and Nanofibers*; Cambridge University Press: Cambridge, U.K., 2014.
(19) Lee, M. W.; An, S.; Jo, H. S.; Yoon, S. S.; Yarin, A. L. Self-healing Nanofiber-Reinforced Polymer Composites. 2. Delamination/Debonding, and Adhesive and Cohesive Properties. *ACS Appl. Mater. Interfaces* **2015**, DOI: 10.1021/acsami.5b03470.
(20) Khansari, S.; Sinha-Ray, S.; Yarin, A. L.; Pourdeyhimi, B. Stress-Strain Dependence for Soy-Protein Nanofiber Mats. *J. Appl. Phys.* **2012**, *111*, 044906.
(21) Sinha-Ray, S.; Khansari, S.; Yarin, A. L.; Pourdeyhimi, B. Effect of Chemical and Physical Cross-Linking on Tensile Characteristics of Solution-Blown Soy Protein Nanofiber Mats. *Ind. Eng. Chem. Res.* **2012**, *51*, 15109−15121.
(22) Khansari, S.; Sinha-Ray, S.; Yarin, A. L.; Pourdeyhimi, B. Biopolymer-Based Nanofiber Mats and Their Mechanical Characterization. *Ind. Eng. Chem. Res.* **2013**, *52*, 15104−15113.
(23) Sinha-Ray, S.; Yarin, A. L.; Pourdeyhimi, B. Meltblown Fiber Mats and Their Tensile Strength. *Polymer* **2014**, *55*, 4241−4247.
(24) Sahu, R.; Sinha-Ray, S.; Yarin, A. L.; Pourdeyhimi, B. Drop impacts on electrospun nanofiber membranes. *Soft Matter* **2012**, *8*, 3957−3970.
(25) Kim, M.-S.; Shin, H.-J.; Park, Y.-K. Measurement of Nonlinear Mechanical Properties of PDMS Elastomer. *Microelectron. Eng.* **2011**, *88*, 1982−1985.
(26) Southwest Airlines Information Regarding Flight 2284. http://www.blogsouthwest.com/news/southwest-airlines-information-regarding-flight-2294/; Aviation Safety Network http://aviation-safety.net/database/record.php?id=20110401-0.

DOI: 10.1021/acsami.5b05998
ACS Appl. Mater. Interfaces 2015, 7, 19546−19554